International Journal of Engineering Research & Technology (IJERT)
ISSN: 2278-0181
Vol. 1 Issue 8, October - 2012

The Design and Fabrication of Low Speed Axial-Flow Compressor Blades by Joukowski Transformation of a Circle

Chigbo A. Mgbemene
Department of Mechanical Engineering, University of Nigeria, Nsukka

Abstract

The design and fabrication of low speed axial flow compressor blades has been carried out. The blade base profile design was done using the Joukowski conformal transformation of a circle. Three sets of blades at three different blade camber angles $\theta = 20^o$, 35^o and 50^o were then fabricated from the base profile out of compressed paper. The blades were tested in a simple smoke tunnel. The results showed that the degree of flow separation from the blade surface is affected by the curvature of the blade. The 20^o blade gave the best performance. This work was done to arouse the minds of young readers towards blade design, particularly the readers in different parts of the world where there is inadequate teaching equipment for students to really put to test what they had been taught in class.

Keywords: airfoil, blade base profile, curvature, flow separation, Joukowski transformation.

1.0 Introduction

The performance of gas turbine systems depends on the efficiency of its compressor and particularly on the performance of the compressor blades. The efficiency of a compressor is basically determined by the smoothness of the air flowing through it. In the axial flow compressor, the basic components used in the flow path of the compressor are the rotor blades and the stator blades. These are shaped in the form of airfoils (Fig. 1) to maintain the smoothest airflow possible. The angle at which the air flows across these airfoil shapes is critical to performance of the system.

The design of these blade shapes is critical. It demands the consideration of many variables in relation to the system, blade shape and operational condition. Blades must be designed to have correct aerodynamic shape and also be light, tough, and not prone to excessive noise and excessive vibrations. Blades must also be designed to achieve substantial pressure differentials per stage. In this case, the blade curvature has a large part to play. The shape of the blades determines the amount of power that could be generated from a gas turbine system. The shape also determines the amount of loading and stresses which the blades will endure and in fact; a host of other effects on the gas turbine system are linked to the blade curvature [1, 2, and 3].

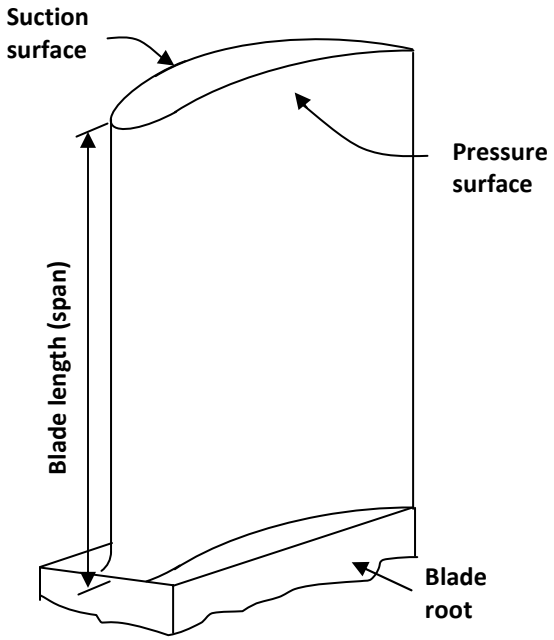

Fig. 1: A typical axial-flow compressor blade.

In recent times there have been some sophisticated ways for designing the blade shape, for example, the T-AXI, a new turbomachinery design system developed by Mark, et al [4]. Several of such methods have been developed by the major engine manufacturers but they have kept them proprietary for competitive reasons [1]. Due to this fact, it is difficult for the students and young engineers, particularly, in the developing world (who still have to contend with the need for basic infrastructures before thinking of advanced educational facilities) to obtain specific data for blade designs. Many a young engineering graduate in the developing world therefore, thinks that the development of gas turbine engine is an impossible task particularly in the development of the blades. This paper hopes to present a rudimentary way of designing the gas turbine blades without the use of the sophisticated software. It also hopes to arouse in the minds of the young readers that the development of the gas turbine compressor blade, albeit for conducting basic experiments, can be achieved. The subsequent test of the blades will demonstrate that the designed blades behaved as such blades were supposed to behave.

The base profile can be constructed or can be determined from the Joukowski transformation of a given circle.

This work is basically to design axial-flow compressor blades at three different camber angles using the Joukowski conformal transformation of a circle. The designed blades were fabricated and basic flow tests were carried out with them. Certain characteristics of blades like the lift and drag coefficients were not determined as this was just a simple demonstrative experimentation.

2.0 Literature review

The development of the airfoil blade shape of the compressor blade could be said to have been pioneered by Alan Arnold Griffith an English engineer. In 1926 he published a seminar paper,

noting that the reason for the poor performance of the existing compressors at that time was because flat blades were used and the blades were essentially "flying stalled". He showed that the use of airfoils instead of the flat blades would dramatically increase efficiency, to the point where a practical jet engine was a real possibility [5].

Since that publication, many experiments and works have studied the operation of single stage fans and compressors at different flow conditions but these studies revolved mainly around stalling and surging of compressors. Notable names like Frank Whittle an Englishman, Pabst von Ohain a German; the United States' National Advisory Committee on Aeronautics (NACA) and National Aeronautics and Space Administration (NASA), the British National Gas Turbine Establishment (NGTE) have made serious developments in the compressor blade shape as we have them now.

Details about the design of blades abound in literatures such as in [1, 6, 7, and 8]. The use of Computational Fluid Dynamics (CFD) in the design of blades has been reviewed by Horlock and Denton in [9]. Benini [10] reviewed quite some of the recent works done in the blade design. Egartner and Schulz [11] developed a computer package OptiMISES which is basically stream surface optimization that will help reduce the turnaround times for turbo machinery design. The software helped find quasi-3D-dimensional blade shapes which promised stability and efficiency over the full presumed working range of the blade; while satisfying the constraints arising from aerodynamic, heat transfer, aeromechanical, mechanical and manufacturing considerations. Dang, et al [12] developed a three-dimensional viscous inverse method which allowed blading design with full interaction between the prescribed pressure-loading distribution and a specified transpiration scheme.

The sophistication of the developed packages are way beyond what undergraduates can easily comprehend in their design of the blades hence this need to present them with the simple basic way of blade design. The designed blades here will by no means present very efficient systems but it would be enough to get the students going in blade designs.

2.1 Evaluation of the blade profile: In the axial-flow compressor, compression of air is achieved by first accelerating the air and then diffusing it to obtain a pressure increase. The air is accelerated by a row of rotating airfoils (blades) called the rotor, and then diffused in a row of stationary blades (the stator). According to Cohen [1] two major requirements of the blade row, whether rotor and stator, are to turn the air through the required angle $(\beta_1 - \beta_2)$ in case of the rotor and $(\alpha_2 - \alpha_3)$ in the case of the stator; and secondly, carry out diffusing process with optimum efficiency i.e. with minimum loss of stagnation pressure. These can be achieved due to the geometry of the blade profile. The blades are curved.

According to [13] a blade profile could be defined by:

(a) The blade maximum thickness
(b) The position of the blade maximum thickness
(c) The camber-line
(d) The position of the blade maximum camber
(e) The thickness of the leading and trailing edges.

But they also noted that these five quantities do not completely define the profile. These quantities can be chosen purely on aerodynamic grounds with the exception of the blade maximum thickness and the trailing-edge thickness. The blade maximum thickness is closely associated with the mechanical strength of the blade and is not available for the control of the section aerodynamics of the blade. Carter, et al [13] further pointed out that however; brief tests on leading-edge and trailing-edge thickness suggest these have only a minor effect on the aerodynamic performance provided the trailing-edge thickness is not allowed to become excessive. Sharper leading-edges seemed beneficial at high speeds, but the gain is small. Indeed, circular leading edges are more beneficial for low speed flow situations which are what could only be achieved in the university laboratory where the design was carried out. In this design, the position of maximum camber and maximum thickness as major variables controlling the aerodynamic performance will be considered for the reasons presented in [13].

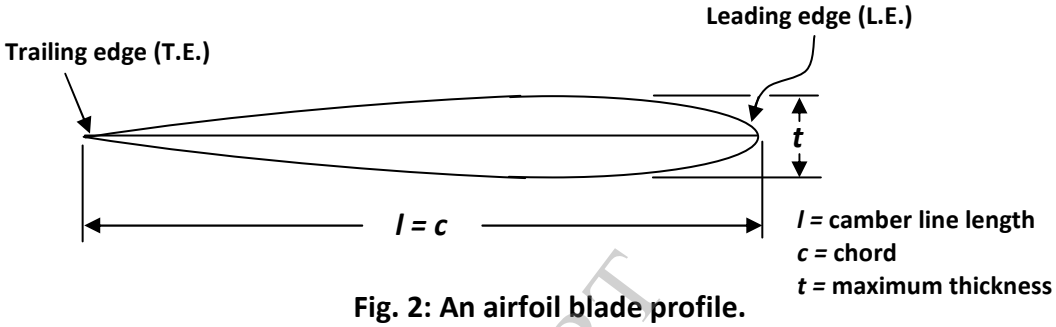

Fig. 2: An airfoil blade profile.

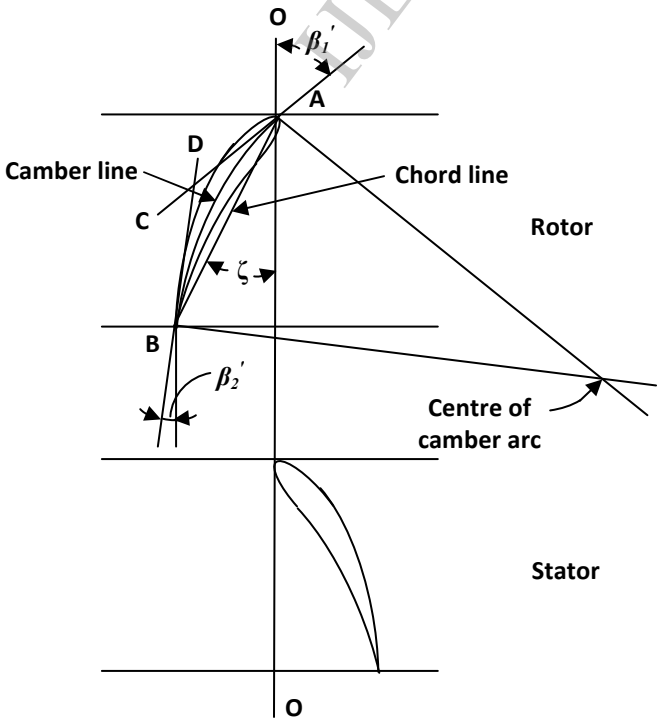

Fig. 3: The curved blade notations.

The design of the blade starts with the construction of the blade base profile (Fig. 2). The base profile can be defined as the basic shape of an airfoil with a straight camber line (where the camber length equals the chord) as shown in Fig. 2.

Since the operational blades are curved in shape, Fig. 3 shows some of the notations for defining the geometry of the curved blade. The chord line of an airfoil is a straight line drawn from the leading edge to the trailing edge of the airfoil, and the chord is the length of the chord line. The camber line is a line drawn halfway between the two surfaces. The camber of the blade is defined as the distance between the camber line and the chord line or it could be defined as the ratio of the maximum ordinate of camber line to the chord. The camber angle θ is the turning angle of the camber line. The blade shape is described by specifying the ratio of the chord to the camber at some particular length on the chord line, measured from the leading edge. The aspect ratio AR is the ratio of the blade length (span) to the chord length [2, 14].

According to Perkins in [6], in the design of the blade, the centre of the leading edge radius is usually obtained by drawing a line through the end of the chord with slope equal to slope of camber line at 0.5 percent of chord and laying off the leading edge radius along this line. The position of maximum thickness is always 30 percent of the chord [6, 13]. The ratio of maximum thickness to chord, *(t/c)* for blade shapes is generally 10 percent [2].

Although the blades are designed singly, they do not operate as such. They must operate in rows or cascades with notation as shown in Fig. 4. One fact remains that air will not leave a blade precisely in the direction indicated by the blade outlet angle, factors like velocity of the air and pressure ratio will affect the exit point. For this reason, to obtain a good performance over a range of operating conditions, it is wise not to make the blade angle equal to the design value of the relative air angle.

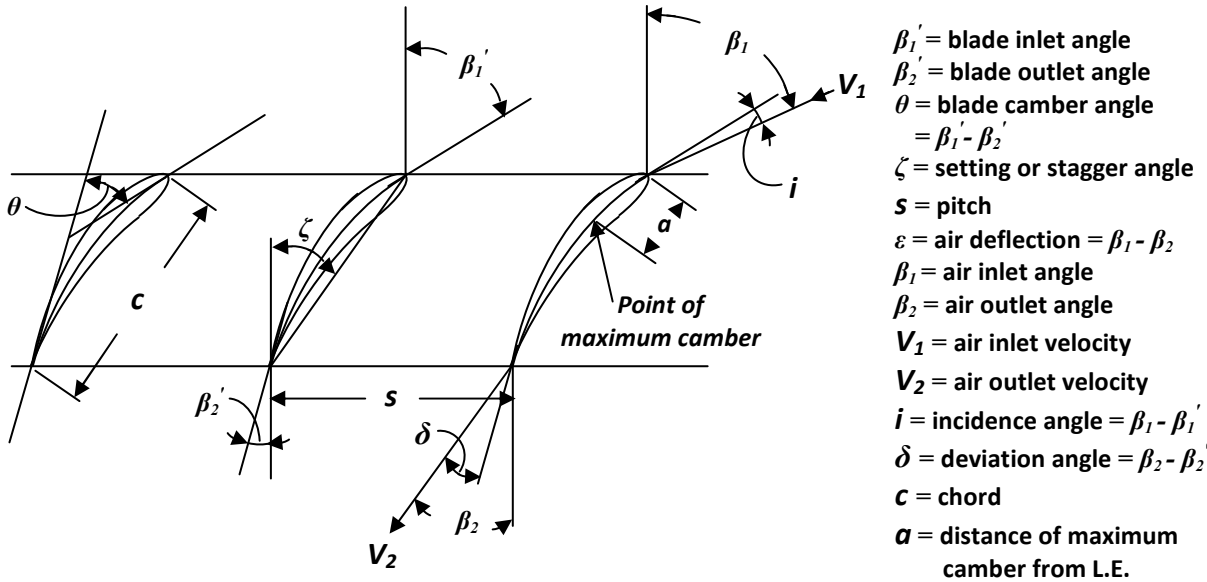

Fig. 4: Compressor cascade and blade notation.

3.0 The blade design by Joukowski transformation of a circle [14, 15, 16, 17]

3.1 The Joukowski airfoil: The base profile of Fig. 2 can be obtained by the transformation of a suitable circle using the generalized Joukowski transformation of order *k* (Eq. 1), where *k* is a positive integer [15].

$$w = f(z) = \frac{1}{2}\left(z^{k} + z^{-k}\right) \tag{1}$$

It maps the unit circle into the interval (-1, 1) of the real axis in the *w*-plane traced *2k* times.

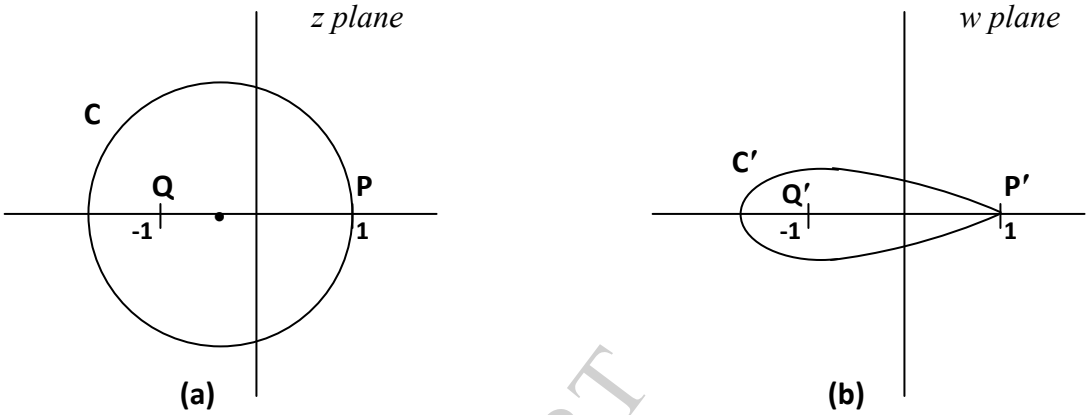

Fig. 5: (a) The circle *C* to be transformed. (b) The airfoil shape *C′* resulting from the transformation of the circle.

Consider a circle *C* in the z-plane having its centre offset from the origin on the real axis, let P and Q be points in the z-plane corresponding to $z = 1$ and $z = -1$ respectively with reference to the origin on the real axis. Also let the circle pass through $z = 1$ and have $z = -1$ as an interior point as shown in Fig. 5(a). The image of *C* can be mapped onto the *w* plane using Eq. (2) which is the same as Eq. (1) with $k = 1$. This mapping transforms suitable circles into airfoils with sharp trailing edges whose interior angles are equal to zero.

$$w = f(z) = \frac{1}{2}\left(z + \frac{1}{z}\right) \tag{2}$$

This mapping is conformal. Differentiating Eq. (2) with respect to *z* we have:

$$\frac{dw}{dz} = \frac{1}{2}\left(1 - \frac{1}{z^{2}}\right) \tag{3}$$

dw/dz vanishes at the points $z = 1$ and $z = -1$ making them critical points. The mapping ceases to be conformal in the immediate neighbourhood of these points. Since $z = -1$ is an interior point, $z = 1$ becomes the main critical point and the vertex is formed here. The point $z = 1$ transforms to $w = 1$. We can obtain this from Taylor series expansion of $f(z) = ½(z + 1/z)$ about $z = 1$.

$$w - 1 = \tfrac{1}{2}\,[(z-1)^2 - (z-1)^3 + (z-1)^4 - \ldots] \qquad (4)$$

By direct transformation of points on *C*, other points on *C′* can be found. The resulting profile of *C′* is of airfoil shape (Fig. 5(b)). From [14] we can see that the angles with vertices at $z = 1$ are doubled under the transformation. Since the angle at z = *1* exterior to *C* is π, the angle at $w = 1$ exterior to *C′* is 2π. Therefore *C′* has a sharp tail at $w = 1$. This forms the base profile which was used for the construction of the blade shape. This airfoil shape is known as the Joukowski airfoil. It is similar to the NACA 4- and 5- series airfoil shapes [6, 18 and 19].

Having obtained the base profile, the construction of the model blades was proceeded to. The resulting base profile (Fig. 5(b)) cannot be used for constructing the blade unless it is calibrated in the manner shown in Fig. 6 with the ordinates being specified [1].

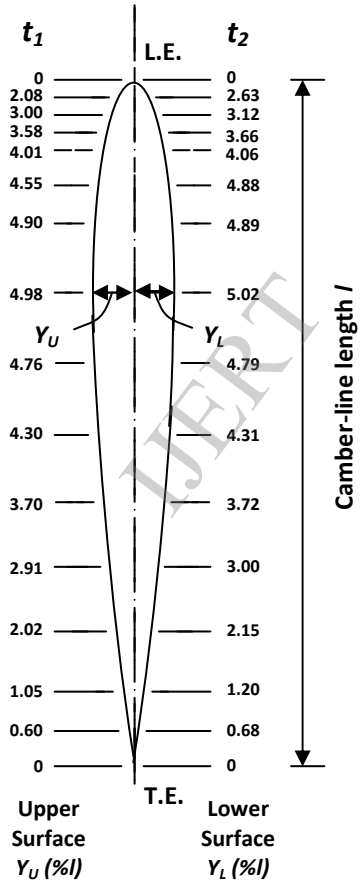

Fig. 6: A calibrated blade base profile [1].

3.2 The blade construction: The ordinates of the base profile t_1 and t_2 are given at definite positions along the camber-line as shown in Fig. 6. With the ordinates known, the value of the Y_U and Y_L are computed as

$$Y_U, Y_L = \frac{t_n \times l}{100} \qquad (5)$$

where t_n = already specified ordinates in Fig. 6 as t_1 and t_2
n = 1 and 2 for upper and lower sections of the profile respectively
l = camber length (chord)

Recall that the centre of the leading edge radius is usually obtained by drawing a line through the end of the chord with slope equal to slope of camber line at 0.5 percent of chord and laying off the leading edge radius along this line; the position of maximum thickness is always 30 percent of the chord and the ratio of maximum thickness to chord *(t/c)* for blade shapes is generally 10 percent, the *Y* values were computed and laid off at calculated points on the *X* axis.

Table 1: The calculated values used for the blade construction

Line from the leading edge	t_1	Y_U (mm)	t_2	Y_L (mm)	Y_U, Y_L located at %*l*	*X* (mm)
0 (L.E)	0.00	0.000	0.00	0.000	0.0	0.00
1	2.08	1.456	2.63	1.841	2.5	1.75
2	3.00	2.100	3.12	2.184	5	3.50
3	3.38	2.506	3.66	2.562	7.5	5.25
4	4.01	2.807	4.06	2.842	10	7.00
5	4.55	3.185	4.88	3.416	15	10.50
6	4.89	3.423	4.90	3.430	20	14.00
7	4.98	3.486	5.02	3.514	30	21.00
8	4.76	3.332	4.79	3.353	40	28.00
9	4.30	3.010	4.31	3.017	50	35.00
10	3.70	2.590	3.72	2.604	60	42.00
11	2.91	2.037	3.00	2.100	70	49.00
12	2.02	1.414	2.15	1.505	80	56.00
13	1.05	0.735	1.20	0.840	90	63.00
14	0.60	0.42.0	0.68	0.476	95	66.50
15 (T.E)	0.00	0.000	0.00	0.000	100	70.00

A chord length of 70mm and a blade length (span) of 100mm were chosen for the sake of handling and the size of the wind tunnel that will be used for the testing. The values were calculated thus:

$$Y_U = \frac{t_1 \times l}{100}$$

$$Y_{U\,2.08} = \frac{2.08 \times 70}{100} = 1.456mm$$

$$Y_L = \frac{t_2 \times l}{100}$$

$$Y_{U2.63} = \frac{2.63 \times 70}{100} = 1.841mm$$

Both $\boldsymbol{Y_U}$ and $\boldsymbol{Y_L}$ are located on X at 2.5% of l

$$= \frac{2.5 \times 70}{100} = 1.75mm$$

The calculated values used for the construction of the blades are given in Table 1.

Having computed the Y, t and X values, a suitable pitch/chord ratio (s/c) of 0.57 (to achieve a high air deflection) [1] and a stagger angle of 34° were chosen. The choices were made based on the actual data from blade samples obtained from gas turbine blades of Afam Power Station Port Harcourt Nigeria which were Asea Brown Boveri gas turbines whose deflection curves agreed with the typical design deflection curve presented in [1]. Since the blades were to be curved, a circular arc camber line was assumed and the blades were constructed for θ = 20°, 35° and 50°. θ is related to β_1', β_2' and ζ thus:

$$\theta = \beta_1' - \beta_2' \quad (6)$$

$$\zeta = \beta_1' - \theta/2 \text{ [1]} \quad (7)$$

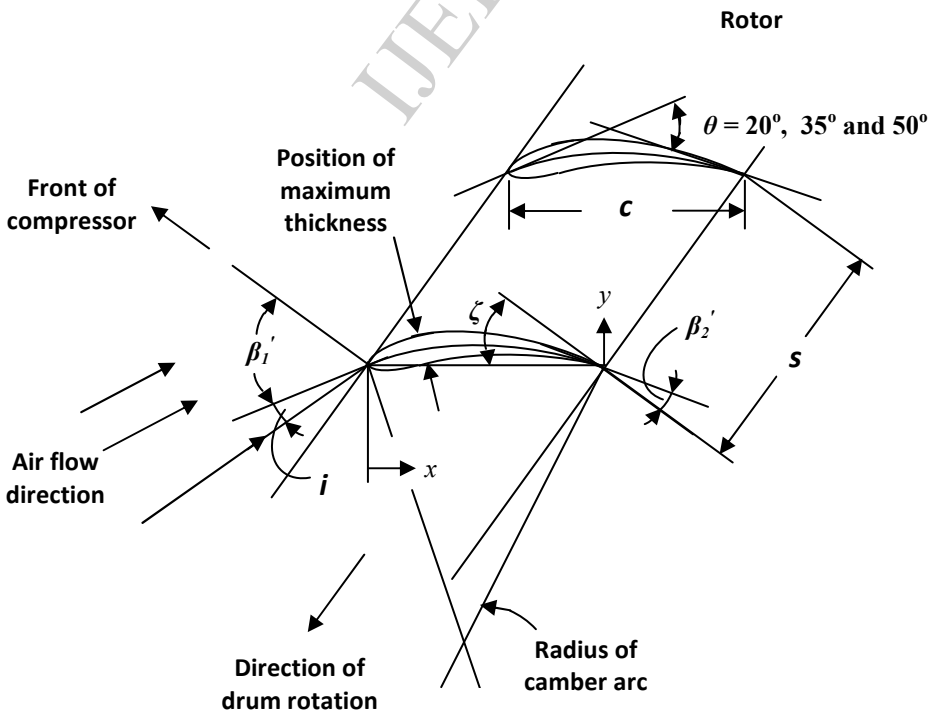

Fig. 7: Blade cascade arrangement for θ = 20°, 35° and 50°

From Eqs. (6) and (7) the following values of β_1' and β_2' for the various values of θ were obtained:

(i) For $\theta = 20^o$ $\zeta = 34^o$, $\beta_1' = 44^o$ and $\beta_2' = 24^o$

(ii) For $\theta = 35^o$ $\zeta = 34^o$, $\beta_1' = 51.5^o$ and $\beta_2' = 16.5^o$

(iii) For $\theta = 50^o$ $\zeta = 34^o$, $\beta_1' = 59^o$ and $\beta_2' = 9^o$

The model blades were fabricated in a like manner as given in [1]. They were made from 1mm thick card board paper and were arranged two blades in a cascade as shown in Fig. 7. Figure 8 shows the model blades which were subsequently tested.

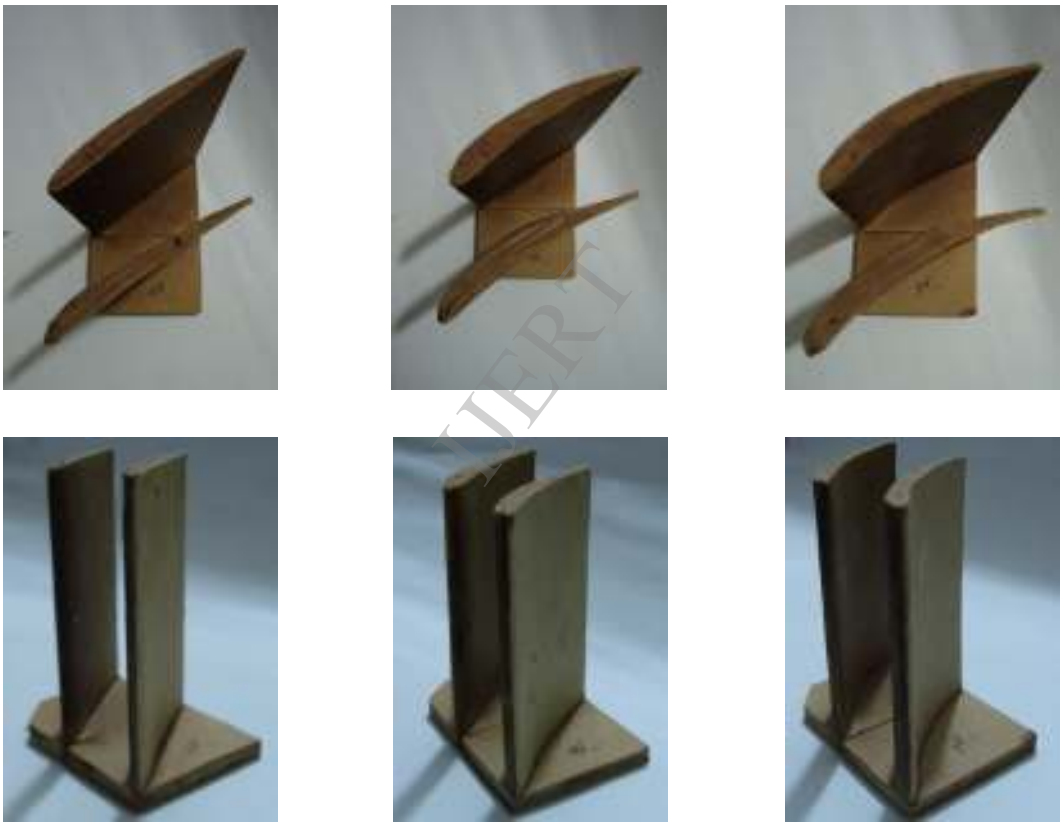

(a) **(b)** **(c)**

Fig. 8: The fabricated blade samples (a) $\theta = 20^o$ (b) $\theta = 35^o$ and (c) $\theta = 50^o$.

4.0 Tests, Results and Discussions

The fabricated blades were tested in a wooden smoke tunnel with white smoke as the working fluid. The observations were visual through a Perspex cover placed over the blade test section.

The smoke was sucked through the blade cascade arrangement by a hand-held fan placed at the end of a chimney connected to the test chamber. The fan was run at three different speeds:

(i) N. speed (NS) – 3.7m/s
(ii) Speed 1 (S1) – 5.2m/s
(iii) Speed 2 (S2) – 10.6m/s.

It was necessary to experiment with low subsonic speeds (not exceeding 15m/s) so as to maintain laminar flow of the smoke over the airfoils. At high speeds diffusion of smoke occurs.

The behaviour of flow over the blades was observed for each blade set and the results tabulated (Tables 2 - 4) and some specific data plotted (Fig. 9).

Table 2: Values obtained from the $\theta = 20^o$ blade sample test.

20^o specified angle ($i = 0^o$)

S/N	N. Speed (N.S)		Speed1 (S1)		Speed 2 (S2)	
	Point of separation from L.E. (x mm)	Vortex height from suction surface at T.E. (y mm)	Point of separation from L.E. (x mm)	Vortex height from suction surface at T.E. (y mm)	Point of separation from L.E. (x mm)	Vortex height from suction surface at T.E. (y mm)
1	60	5	53	6	47	7
2	64	2	54	4	48	5
3	61	3	55	4	48	2
4	66	1	56	1	49	4
5	70(none)	0	56	3	49	2
6	70(none)	0	57	1	50	2
Average	65.2	1.8	55.2	3.2	48.5	3.7

Table 3: Values obtained from the $\theta = 35^o$ blade sample test.

35^o specified angle ($i = 0^o$)

S/N	N. Speed (N.S)		Speed1 (S1)		Speed 2 (S2)	
	Point of separation from L.E. (x mm)	Vortex height from suction surface at T.E. (y mm)	Point of separation from L.E. (x mm)	Vortex height from suction surface at T.E. (y mm)	Point of separation from L.E. (x mm)	Vortex height from suction surface at T.E. (y mm)
1	47	3	43	7	38	8
2	44	4	44	6	38	6
3	45	5	44	6	41	5
4	46	4	45	6	39	7
5	46	4	45	5	40	6
6	48	2	46	4	40	6
Average	46.0	3.7	44.5	5.7	39.3	6.7

Table 4: Values obtained from the θ = 50° blade sample test.

50° specified angle (i = 0°)

S/N	N. Speed (N.S)		Speed1 (S1)		Speed 2 (S2)	
	Point of separation from L.E. (x mm)	Vortex height from suction surface at T.E. (y mm)	Point of separation from L.E. (x mm)	Vortex height from suction surface at T.E. (y mm)	Point of separation from L.E. (x mm)	Vortex height from suction surface at T.E. (y mm)
1	44	5	40	10	32	12
2	42	6	36	11	32	11
3	41	8	38	10	28	14
4	40	9	38	10	26	16
5	42	7	40	9	30	11
6	44	6	40	9	32	12
Average	42.2	6.8	38.7	9.8	30.0	12.7

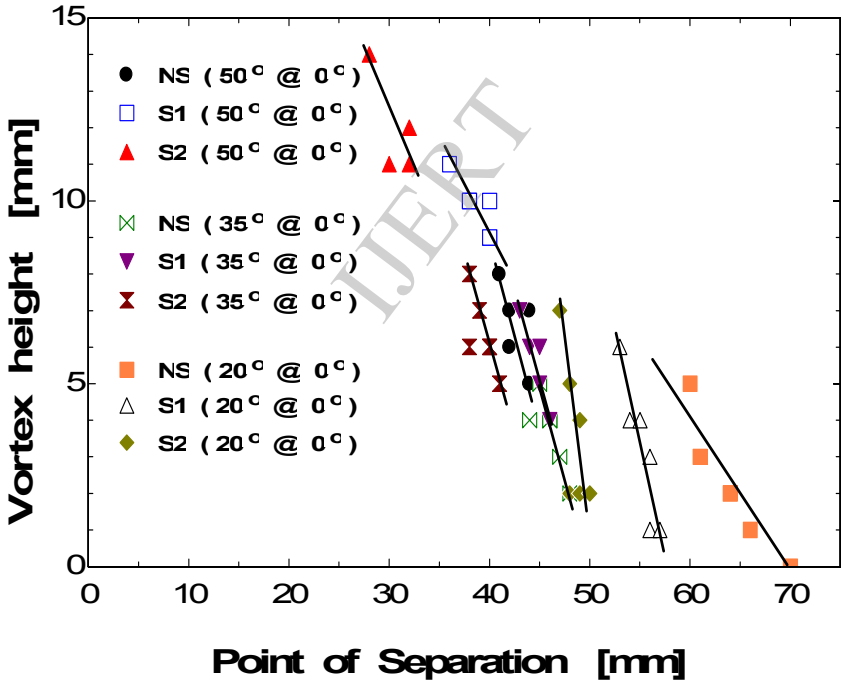

Fig. 9: A plot of Point of Separation against Vortex Height for the (a) θ = 20°, (b) θ = 35° and (c) θ = 50° blade sets at i = 0°.

The experiment was just a simple one - to study the pattern of air flows through the blade arrangements. The points of air separation from the blade surfaces were measured and the patterns of air separation studied in order to discover the major parameters that affected air flow behaviour. The formation of vortices was also looked out for, and even though the strengths of the vortices were not clearly observable from the flow, their heights were recorded.

The flow around the blade sets were characterized by separations from the blade surface and formation of vortices at the trailing edges. Although the paper did not discuss the mechanism of separation or that of vortex formation, it showed that there is a direct relationship between the two of them. The results showed that for a laminar flow field a linear relationship exists between the point of separation of the flow over an airfoil and the height of the vortex formed at the trailing edge.

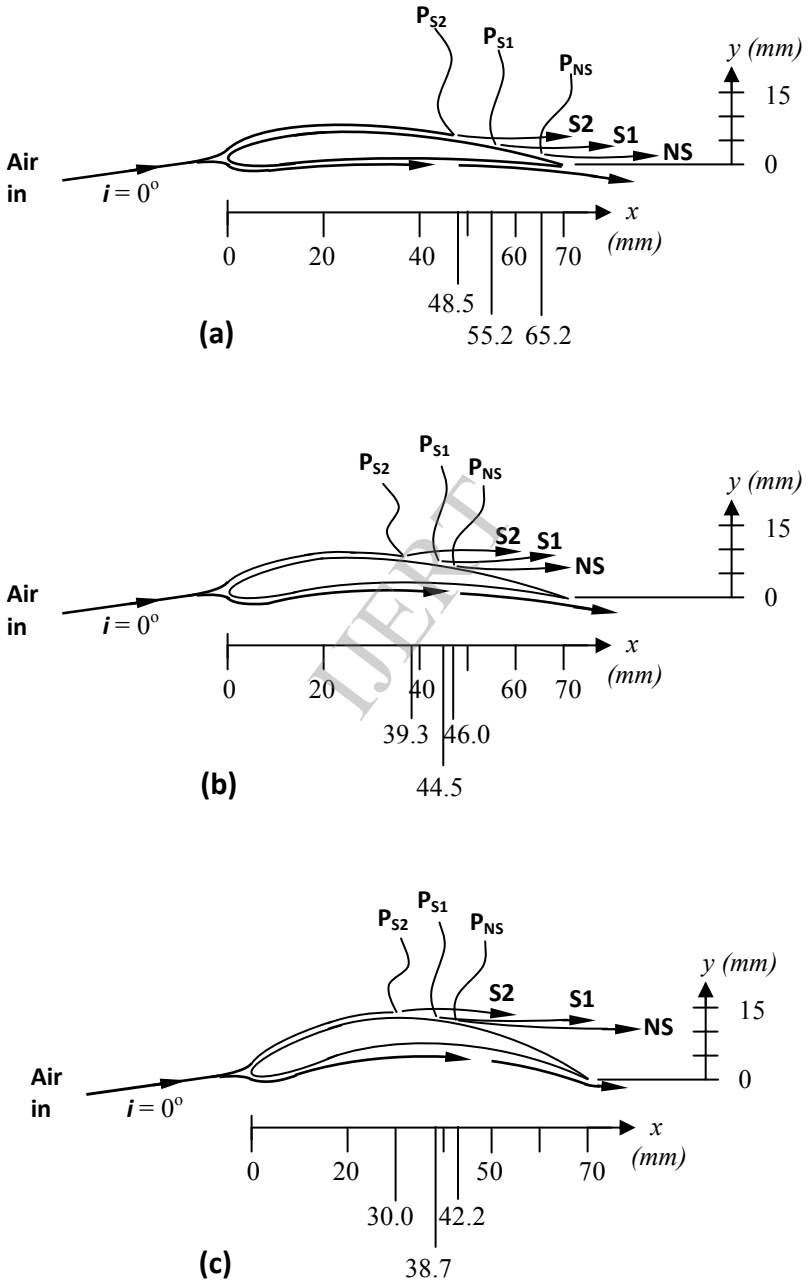

Fig. 10: Points of separation $P_{NS, S1, S2}$ (x axis) and vortex heights (y axis) for the (a) $\theta = 20^o$, (b) $\theta = 35^o$ and (c) $\theta = 50^o$ blade sets.

A look at the result tables ((Tables 2 - 4) and the figures (Figs. 9 and 10) presented some more of interesting facts:

The effect of variation of flow speed: At lower speeds, the flow separations occurred at a longer distance from the leading edge than at the higher speeds. This implies that the air particles have better ability to negotiate around obstacles and as the speeds increased air gradually lost its ability to negotiate curves and then separated from the blade surface. Separation of flow occurs when the boundary layer has traveled far enough against an adverse pressure gradient such that its energy level drops to a level that the boundary layer speed relative to the object falls almost to zero, the flow then detaches from the object and leaves in form of vortices and eddies.

The effect of air velocity variation is more noticeable when one compares the difference in the average separation points. NS is about 71 percent of S1 while S1 is about 52 percent of S2, the about 40 percent increase in speed from NS to S1 causes (on the average of the three blade sets) a 19.5 percent early flow separation and nearly 80 percent increment in the vortex height; while the 100 percent increase in speed from S1 to S2 only causes (on the average of the three blade sets) a 9 percent early flow separation and a 16 percent increase in the vortex height.

Effect of the curvature on the behaviour of the flow: The separations observed on the blades are affected by the degree of curvature of the blade. The deeper the curvature, the more the separation observed in the flow. In the case of $\theta = 20^o$ (Table 2), there were some times the flow never separated from the blade and joined up smoothly at the trailing edge. The average point of separation from the blade was very sensitive to the 15^o curvature increase of the blade from 20^o to 35^o more than it was in from 35^o to 50^o as could be observed from the Tables 2 – 4 and Fig. 10. This reaction does not clearly correspond to the same result with respect to the vortex heights.

From the results, it could be said that increment in the flow speed is not as detrimental to the performance of the blades as the increment in the curvature. As the curvature increased, the point of separation advanced towards the leading edge and the vortex height increased leading to loss of power and its attendant losses.

Looking at the tables and the figures, and comparing the points of separations and the vortex heights, the $\theta = 20^o$ proves to be the best of the three angles compared but although it was the best of the three curvatures, the flow still left the blade surface 30 percent short of the trailing edge. This could have arisen due to the imperfections on the surface of the blade and the angle of incidence of air on the blade.

Comparing Fig. 10 with Fig. 11, it could be seen that the flow around the model blades behaved as was expected of blades in such flow fields. It could be seen that separation from the suction surface of the airfoil of Fig. 10(a) started closer to the trailing edge which agrees with that at zero angle of attack (Fig. 11(a)). Looking at Fig. 10(c), the close resemblance to Fig. 11(b) could also be observed. Here the large curvature has the same effect as a blade set at high angle of attack. This high angle of attack always resulted in early separation of the flow from the surface and the consequent increase in drag over the surface.

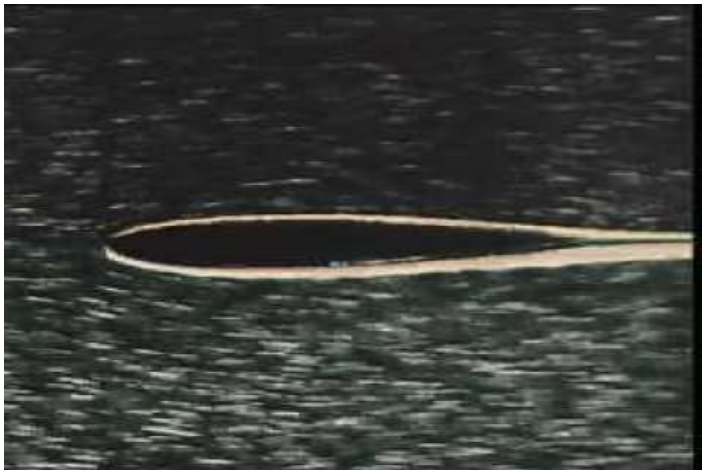

(a)

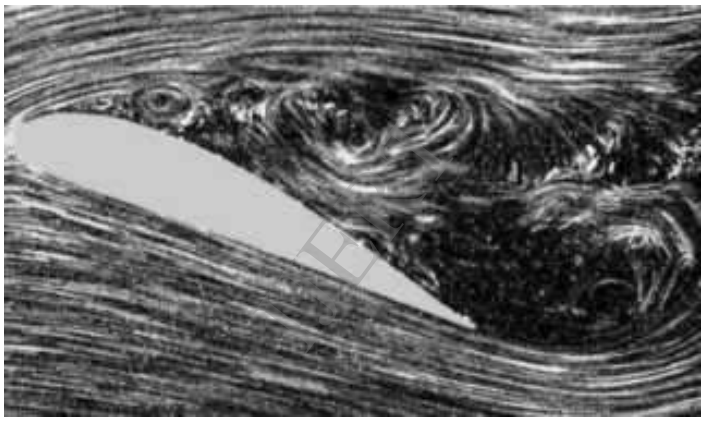

(b)

Fig. 11: Airflow separating from airfoils at (a) zero angle of attack and (b) high angle of attack [20, 21].

5.0 Conclusions

Axial-flow compressor blades have been designed using the Joukowski conformal transformation of a circle and three cascade sets have been fabricated at three different camber angles. The use of Joukowski conformal transformation of a given circle makes it less cumbersome in the design of the blade. The alternative would have been by geometric construction of the base profile in the absence of sophisticated design software. The designed blades were subjected to basic flow tests. The subsequent tests of the fabricated blades have demonstrated that the designed blades behaved as such blades were supposed to behave.

These results have demonstrated that the blades made the air flow in the way it was presumed but the sharp reaction to the curvature between 20^o and 35^o was not expected. This study has shown that in designing axial compressor blades, shallow angles hold a better promise in the performance of the compressor unit as could be seen from the $\theta = 20^o$ results .

Finally, by these, it has been shown that the development of the gas turbine compressor blade can be achieved. It is hoped to have challenged the young inexperienced minds to try developing gas turbine blades.

References

1. Cohen, H., Rogers, G. F. C. and Saravanamuttoo, H. I. H., 1988, *Gas Turbine Theory*, 3rd Ed., Longman Scientific and Technical, Harlow Essex, UK, Chap. 4.
2. Boyce, Meherwan P., 2002, *Gas Turbine Engineering Handbook*, 2nd Ed., Gulf Professional Publishing, Boston, Chap. 7
3. Mgbemene, C. A., 2002, "The Effect of Blade Curvature in the Failure of Gas Turbine Blades," M.Eng. Thesis, University of Nigeria, Nsukka, Enugu State.
4. Turner, M. G., Merchant, A. and Bruna, D., 2006, "A Turbomachinery Design Tool For Teaching Design Concepts for Axial-Flow Fans, Compressors and Turbines," *Proc. of GT2006 ASME Turbo Expo 2006*, Barcelona, Spain, pp 1 - 16.
5. Anonymous, 2011, "Axial Compressor," *Wikipedia* [online], http://en.wikipedia.org/wiki/Axial_compressor, accessed 29 Dec. 2011
6. Perkins, C. D. and Hage, R. E., 1958, *Airplane Performance Stability and Control*, John Wiley & Sons, Inc., New York, Chap. 2.
7. Dixon, S. L., 1998, *Fluid Mechanics and Thermodynamics of Turbomachinery*, 4th Ed., Butterworth- Heinemann, Boston, Chap. 5.
8. Horlock, J. H., 1958, *Axial Flow Compressors*, Butterworths Scientific Publications, London.
9. Horlock, J. H. and Denton, J. D., 2005, "A Review of Some Early Design Practice Using Computational Fluid Dynamics and a Current Perspective," *ASME Journal of Turbomachinery*, **127**, pp 5 – 13.
10. Benini, E., Advances in Aerodynamic Design of Gas Turbines Compressors, http://www.intechopen.com/source/pdfs/12083/InTech-Advances_in_aerodynamic_design_of_gas_turbines_compressors.pdf, accessed 6 Jan. 2012.
11. Egartner, W. and Schulz, V., 1999, "Turbine and Compressor Blade Profile Optimization," http://egartner.de/turbo.html, accessed 30 Dec. 2011.
12. Dang, T. Q., Van Rooij, M. and Larosiliere, L. M., 2003, "Design of Aspirated Compressor Blades using Three-Dimensional Inverse Method," NASA/TM—2003-212212, ARL–TR–2957, GT–2003–38492, http://gltrs.grc.nasa.gov/, accessed 31 Dec. 2011.
13. Carter, A. D. S., Turner, R. C., Sparkes, D. W. and Burrows, R. A., 1960, "The Design and Testing of an Axial-Flow Compressor having Different Blade Profiles in Each Stage," Reports and Memoranda, Ministry of Aviation, Aeronautical Research Council, London, *A.R.C. Technical Report* No. 3183.
14. Milne-Thompson, L. M., 1977, *Theoretical Hydrodynamics*, 5th Ed., The Macmillan Press Ltd, London, Chaps. 6 and 7.
15. Cruz, C., Falčao, M. I. and Malonek, H.R., 2011, "3D Mappings by Generalized Joukowski Transformations," *Computational Science and its Applications, Lecture Notes in Computer*

Science, **6784**, pp. 358 - 373. http://repositorium.sdum.uminho.pt/bitstream/1822/15169/1/CruzFalcaoMalonek2011.pdf , accessed 31 Dec. 2011.

16. National Aeronautics and Space Administration, "Conformal Mapping: Joukowski Transformation," http://www.grc.nasa.gov/WWW/K-12/airplane/map.html, accessed 31 Dec. 2011.
17. Spiegel, M. R., 1972, *Shaum Outline Series, Theory and Practice of Complex Variables*, SI (Metric) Ed., McGraw-Hill Book Company, New York, Chap. 8.
18. Hlavka, G. E., 1954, "An Approximate Theory for Potential Flow through Cascades of Airfoils," Ph.D Thesis, California Institute of Technology, Pasadena, California, http://thesis.library.caltech.edu/5013/1/Hlavka_ge_1954.pdf, accessed 2 Jan. 2012.
19. Kapania, N. R., Terracciano, K. and Taylor, S., 2008, "Modeling the Fluid Flow around Airfoils using Conformal Mapping," http://www.siam.org/students/siuro/vol1issue2/S01010.pdf, accessed 2 Jan. 2012.
20. Bakker A., 2002, "Applied Computational Fluid Dynamics," *Lecture 11 – Boundary Layers and Separation*, http://www.bakker.org/dartmouth06/engs150/11-bl.pdf, accessed 16 Jan. 2012
21. Anonymous, 2012, "Flow Separation," *Wikipedia* [online], http://en.wikipedia.org/wiki/File:Flow_separation.jpg, accessed 16 Jan. 2012.